# Boosting sodium-ion batteries performance by N-doped carbon spheres featuring porous and hollow structures

Ying Yang [a], Tao Deng [a], Xuyuan Nie [a],Huaiyu Wen [a], Liuyue Cao[b,c*], Shigang Sun[a,d], Binwei Zhang[a*]

[a] *Center of Advanced Electrochemical Energy (CAEE), Institute of Advanced Interdisciplinary Studies; State Key Laboratory of Advanced Chemical Power Sources, School of Chemistry and Chemical Engineering, Chongqing University, Chongqing, 400044, China.*

[b] *College of Materials Science and Engineering, Chongqing University, China.*

[c] *School of Chemical Engineering, UNSW Sydney, 2052, Australia*

[d] *State Key Laboratory of Physical Chemistry of Solid Surfaces, Department of Chemistry, College of Chemistry and Chemical Engineering, Xiamen University, Xiamen 361005, China.*

**Synthesis of polydopamine wrapped $SiO_2$ spheres (PDA@$SiO_2$)**

First, $SiO_2$ spheres were prepared via the sol-gel method. Specifically, a hybrid solution comprising 5 mL of ammonia, 30 mL of deionized water, and 100 mL of ethanol was mixed and stirred for 30 minutes. Following this, 5 ml of tetraethyl orthosilicate (TEOS) was added into the mixture and stirred for an additional hour to form $SiO_2$ spheres. Next, 0.3 M dopamine hydrochloride solution was gradually introduced into the $SiO_2$ solution. After 24 hours of reaction, dopamine polymerized to create a polydopamine (PDA) layer on the surface of $SiO_2$ spheres. The resulting mixture was then centrifuged, and the supernatant was removed using deionized water and ethanol. The final product was labelled as PDA@ $SiO_2$.

**Synthesis of NHCSs**

The as-prepared PDA@$SiO_2$ spheres were pyrolyzed in a tube furnace under a programmed heating process, first at 400 ℃ for 2 hours and then at 800 °C for 3h. After naturally cooling to room temperature, the carbonized samples were immersed in a 2M NaOH solution for 4 days to completely remove the $SiO_2$ template and form a hollow structure. Following the alkali etching, the carbon spheres were separated by centrifugation, and washed multiple times with water and ethanol to eliminate any residual alkali and impurities. Finally, the pure hollow N-doped carbon spheres were obtained after drying and labelled as NCHSs.

Purestar PHC-290, purchased from Jiangsu Purestar Environmental Technology Co., Ltd., is a biomass-based SIB anode material known for its excellent cycling stability, discharge efficiency and moisture resistance. Kuraray-Type 2, purchased from Shenzhen Huaqing New Material Technology Co., Ltd.v, is a natural plant-based anode material for SIBs, characterized by high moisture resistance and wider interlayer spacing.

**Structural characterization**

Surface morphology was observed using scanning electron microscopy (SEM) on a Sigma 300. Microstructural information was acquired through transmission electron microscopy (TEM) using an FEI Talos F200X. X-ray diffraction (XRD) was conducted with a SmartLab instrument using Cu Kα radiation (λ=0.15418 nm) over a 5° to 90° range at a scanning rate of 5°$min^{-1}$. The surface chemical composition was investigated by X-ray photoelectron spectroscopy (XPS) using a Thermo K-Alpha. Raman spectroscopy was performed with a LabRam HR Evolution instrument to assess the crystallinity and detect defects within carbon materials.

**Electrochemical measurements**

The electrochemical performance of NHCSs was primarily evaluated using a half-cell configuration. The quality of the active substance, the quality of the conductive agent and the type of binder used in the coating of these three materials are the same and the ratio is the same 8:1:1. Specific values are as follows NHCSs, Purestar, and Kuraray is 0.369 mg $cm^{-2}$,0.397 mg $cm^{-2}$ and 0.448 mg $cm^{-2}$. The resulting mixture was uniformly cast onto a copper foil, which was subsequently dried and cut into small discs with a diameter of 1cm. The half-cells were assembled in an Ar-filled glove box to ensure an anhydrous and anaerobic environment, with sodium metal serving as the counter electrode. In order to assemble into a full battery, we chose sodium vanadium phosphate ( NVP ) as the cathode material. First, sodium vanadium phosphate, conductive carbon black and hydroxymethyl cellulose ( CMC ) were mixed in proportion and ground for 30 minutes. Then, pure water was added to prepare the slurry. After mixing evenly, the slurry was cast on the carbon-coated aluminum foilto form a positive film electrode. The preparation process of the negative electrode was the same as that of half cell, and the porous nitrogen-doped hollow carbon sphere (NHCSs) was used as the negative electrode material. Finally, we assembled the NVP positive electrode and NHCS negative electrode into a full batter. We assembled a full battery with a positive and negative electrode mass ratio of about 2.21. Before this, we first cycled the negative electrode material for 50 cycles, waiting for stability before assembling the full battery. The electrolyte we used is 1.0 M $NaClO_4$ in EC: PC = 1 : 1 Vol% with 5.0 % FEC.

Galvanostatic charge-discharge tests were conducted using a Neware battery test system inside a constant temperature chamber. Cyclic voltammetry (CV) and electrochemical impedance spectroscopy (EIS) measurements were carried out using a Chenhua electrochemical workstation. Galvanostatic intermittent titration technique (GITT) was conducted with a pulse current of 50 $mAg^{-1}$ for 30 min, followed by an interval of 3 hours, and the diffusion coefficients were calculated according to Fick's second law.

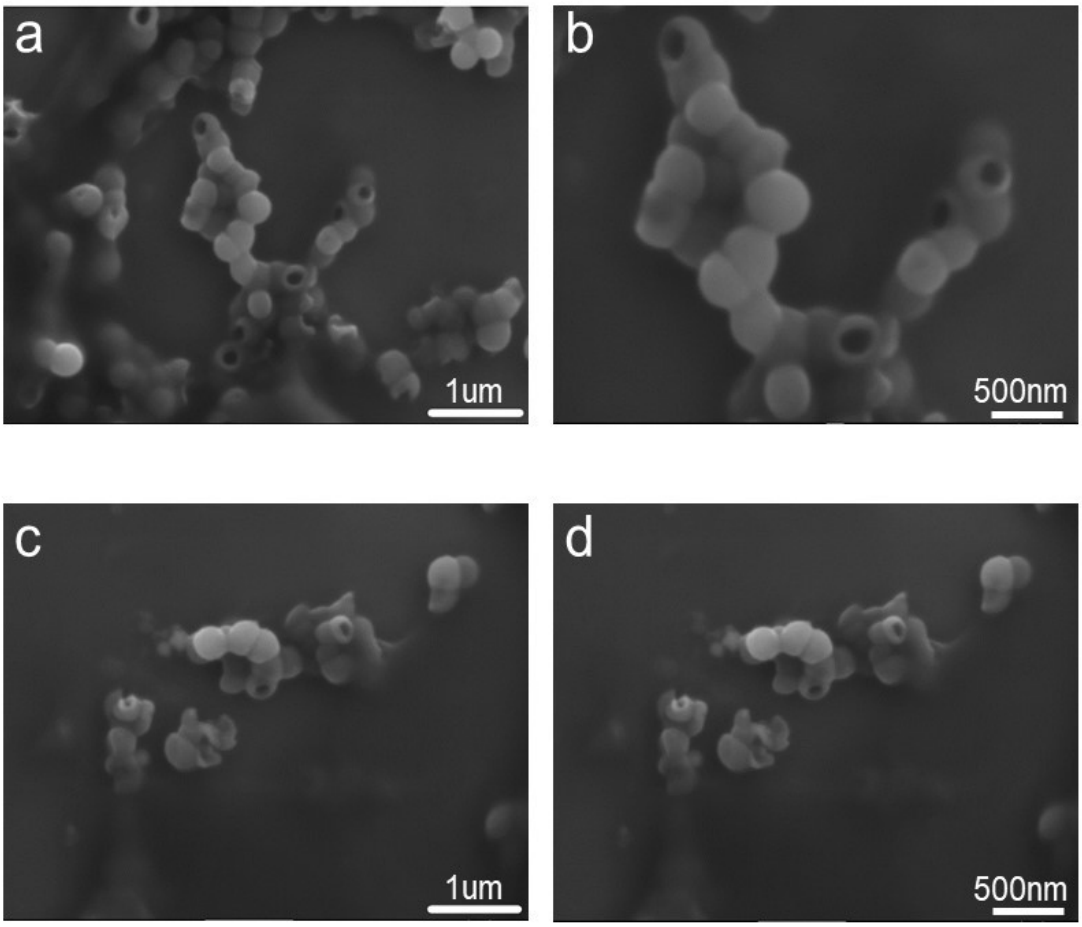


**Fig. S1** SEM images of NHCSs.

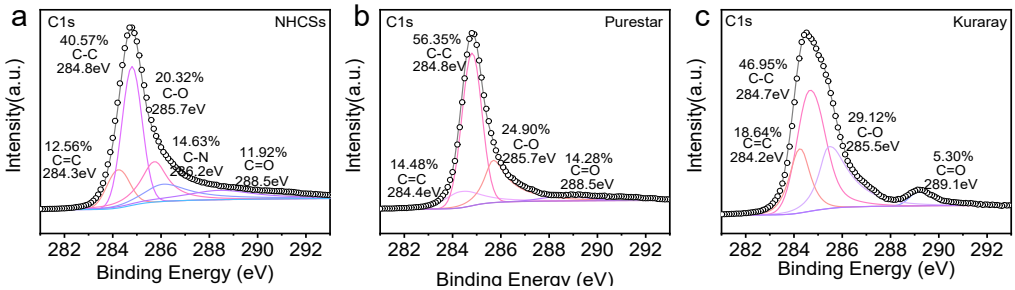


**Fig. S2** The C 1s XPS spectra of NHCSs, Purestar and Kuraray.

The higher ICE of NHCSs, despite their larger surface area and higher disorder compared to Purestar and Kuraray, can be explained by a combination of factors related to surface chemistry and material structure. Typically, a larger surface area increases the extent of SEI formation, which can lower ICE by consuming more charge in the initial cycles. However, NHCSs demonstrate an optimized surface chemistry with fewer oxygen-containing functional groups (Figure S2), which reduces the excessive electrolyte decomposition that usually occurs on carbon surfaces. Moreover, NHCSs have a high proportion of graphitic-N, which is less reactive with electrolytes compared to pyrrolic-N or pyridinic-N, thus contributing to a more stable SEI formation and preserving more active sodium ions for reversible reactions.

Additionally, the hollow and porous structure of NHCSs allows for better electrolyte penetration and sodium ion transport, leading to more efficient ion adsorption and desolvation at the interface, further minimizing unnecessary reactions during the first cycle. This optimized balance between surface area, pore structure, and nitrogen doping enhances both the ICE and overall electrochemical performance.

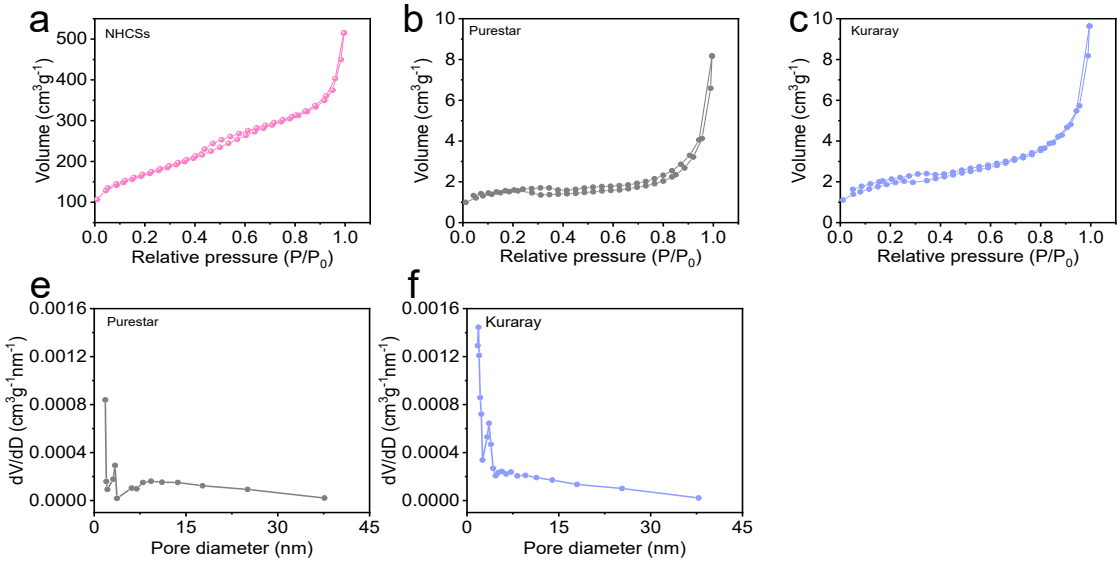


**Fig. S3 (a-c),** Nitrogen adsorption desorption isotherm of NHCSs, Purestar, and Kuraray. **(e-f),** The particle size distribution of Purestar, and Kuraray.

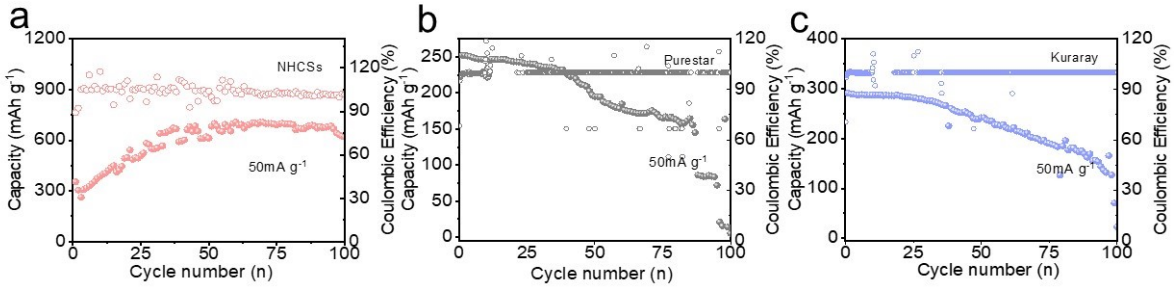


**Fig. S4** Constant current charge and discharge of NHCSs, Purestar and Kuraray battery at 50mAh $g^{-1}$.

The initial capacity increase in capacity observed during the early cycles can be attributed to the gradual infiltration of the electrolyte into the porous and hollow NHCSs structure (Fig. S4a). In the first few cycles, only the outer surface of the NHCSs may have participated in the electrochemical reactions, leading to relatively lower capacity. As cycling progresses, the electrolyte slowly penetrates deeper into the hollow structure, increasing the effective surface area available for $Na^+$ adsorption, which enhances the capacity up to approximately 80 cycles. The slight decrease in capacity afterwards could be attributed to external factors such as temperature fluctuations, and/or electrolyte degradation (e.g., electrolyte decomposition on the Na metal counter electrode side). It's common for batteries to experience some degree of capacity decay over long-term cycling, as the accumulation of side products can impede ion transport or introduce mechanical stress change within the electrode materials, reducing the capacity. In this case, these factors might have played a role in the observed capacity decline. However, we believe the overall stability and performance demonstrated by NHCSs remains better than Purestar and Kuraray both at the same tested current density (as shown in the additional results of Purestar and Kurary in Fig. S4b-4c).

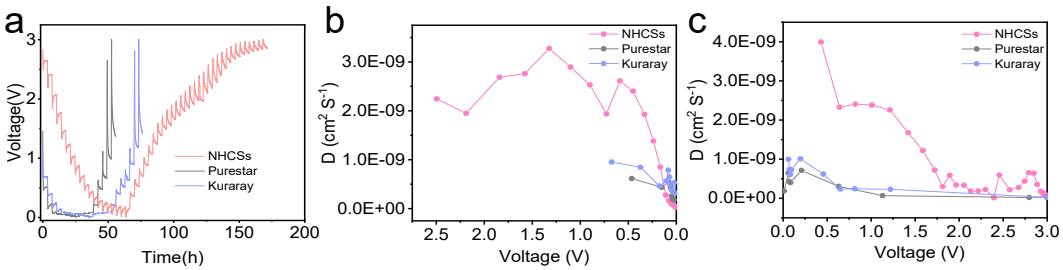


**Fig. S5** GITT charge and discharge curve and sodium ion diffusion coefficient.

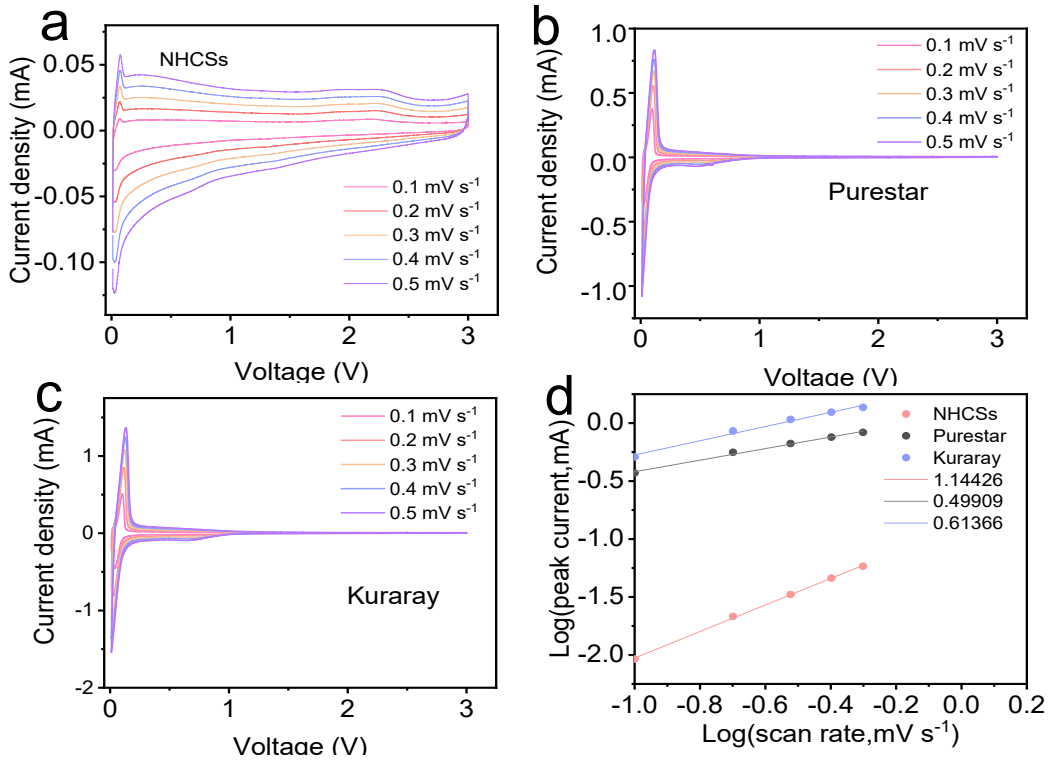


**Fig. S6 Catalytic performance test. (a-c),** CV curves of NHCSs obtained from different scan of 0.1 to 0.5 mV $s^{-1}$ in a symmetric battery. **(d)** The fitting plot of log ( i ) and log ( v ) at the selected peak of CV curve.

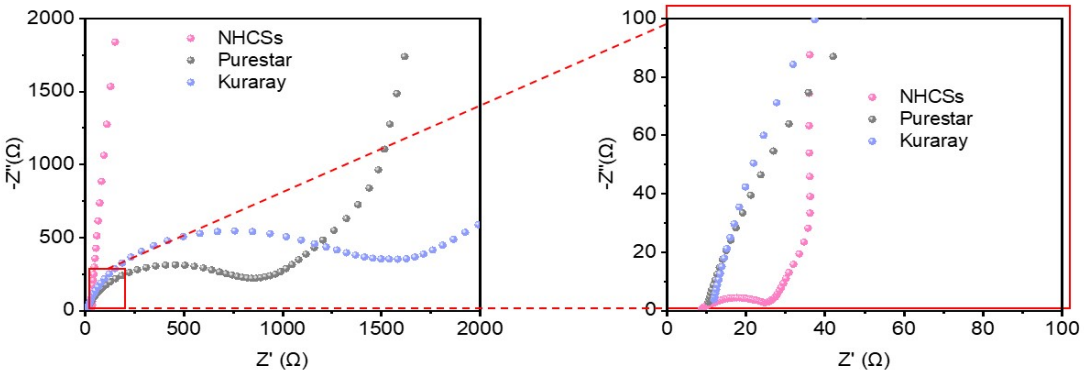


**Fig. S7** The Nyquist diagrams of NHCSs, Purestar, and Kuraray.

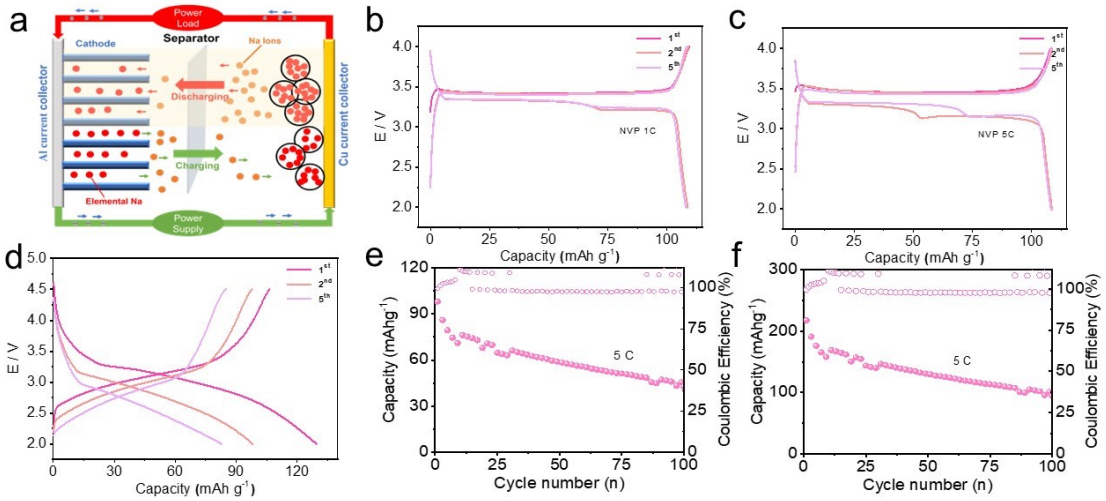


**Fig. S8** (a) The full battery structure diagram of NHCSs. (b-c) The galvanostatic charge-discharge of NVP/Na at 1C and 5C (1C =117.6 mA $g^{-1}$). (d) The galvanostatic charge-discharge of NVP/NHCSs at 5C. (e) The cycle performance of NVP/NHCSs at 5 C (based on the quality of positive electrode). (f) The cycle performance of NVP/NHCSs at 5 C (based on negative electrode mass).

In order to assemble into a full battery, we selected commercial sodium vanadium phosphate ($Na_3V_2(PO_4)_3$, NVP) from YIANTENG SEPCIAL ANODES as the cathode material. To assess the electrochemical performance of the NVP cathode, coin-type half-cells were assembled for charge-discharge testing within a voltage window of 2−4 V, at current densities of 1C and 5C (where 1C = 117.6 mA $g^{-1}$), as shown in Fig. S8b and S8c. The electrolyte used was 1.0 M $NaClO_4$ in EC: PC = 1 : 1 Vol% with 5.0 % FEC. The results show discharge capacities of 109.6 mAh $g^{-1}$ at 1C and 109.2 mAh $g^{-1}$ at 5C, indicating the practicality of the commercial NVP.

The preparation of the anode followed the same process as for the half-cells, with porous nitrogen-doped hollow carbon spheres (NHCSs) used as the anode material. The mass ratio of the cathode to anode was approximately 2.21. The anode was pre-cycled for 50 cycles in a half-cell for pre-sodiation, before being integrated into the full cell. The full cell was tested within a voltage window of 2−4.5 V at a current density of 5C. The first five galvanostatic charge-discharge profiles of the full cell are shown in Fig. S8d, while the cycling performance of the NVP||NHCSs full cell, based on the mass of the positive and negative electrodes, is presented in Fig. S8e and S8f. This full cell

delivered an initial reversible capacity of 218 mAh $g_{NHCSs}^{-1}$ in the first cycle, maintaining 98 mAh $g_{NHCSs}^{-1}$ capacity after 100 cycles, demonstrating the feasibility of using NHCSs.

**Table. S1** The atomic ratios of C, N, O in NHCSs, Purestar and Kuraray.

| Atomic | C 1s | N 1s | O 1s |
|---|---|---|---|
| NHCSs | 89.09% | 4.56% | 6.35% |
| Purestar | 91.86% | 1.19% | 6.95% |
| Kuraray | 87.81% | 0.92% | 11.28% |

**Table. S2** The Particle size and area of NHCSs, Purestar, and Kuraray.

| | D10 (nm) | D50 (nm) | D90 (nm) | D100 (nm) | AREA ($m^2 g^{-1}$) |
|---|---|---|---|---|---|
| NHCSs | 2.00 | 4.88 | 17.40 | 55.20 | 594.38 |
| Purestar | 1.89 | 6.93 | 21.38 | 37.61 | 5.60 |
| Kuraray | 1.93 | 5.15 | 15.94 | 37.83 | 6.94 |

We have measured the tap density (packing density) of NHCSs, Purestar, and Kurary. As expected, NHCSs exhibit a lower tap density due to their highly porous structure (Table S3). However, this architecture of NHCSs also offers unique advantages. The hollow spheres of NHCSs can store significant amounts of electrolyte within the electrode itself, reducing the need for additional space in other cell components for electrolyte storage. This integrated electrolyte storage not only enhances ionic transport and rate performance but also improves the overall volumetric capacity density of the battery. We measured the true density of NHCSs using the water displacement method and found it higher than that of Purestar and Kuraray (Table S3). When combined with the high specific capacity of NHCSs, this results in a much higher volumetric capacity than indicated by tap density alone. In other words, NHCSs can store more capacity in a given volume, especially if the electrolyte storage within the structure is accounted for.

**Table. S3** Densities and corresponding volumetric capacities.

| | NHCSs | Purestar | Kuraray |
|---|---|---|---|
| Tap density ($gcm^{-3}$) | 0.13 | 0.62 | 0.54 |
| True density ($gcm^{-3}$)* | 3.52 | 1.25 | 2.00 |
| Volumetric capacity ($mAhcm^{-3}$)** | 2457.08 | 244.99 | 294.40 |

*Measured through water displacement method

** Calculated by the true density times the specific capacity stabled at 50 $mAhg^{-1}$